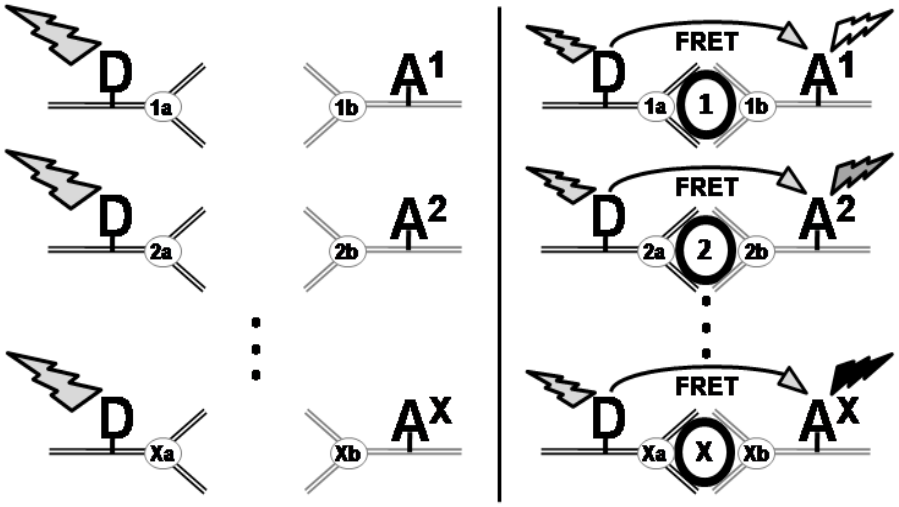

Figure 1: *Homogeneous immunoassays principle with several antibodies (1-X a/b - specific to marker proteins 1-X) labelled with one donor (D) and several acceptors (A^1-A^X) for colour multiplexing.* ***Left:*** *Without protein markers only D exhibits a long-lived luminescence signal after pulsed light excitation (large D-A distance ➔ no FRET).* ***Right:*** *Addition of different proteins leads to specific binding and concomitant specific (colour) long-lived luminescence signals from A^1-A^X (small D-A)*

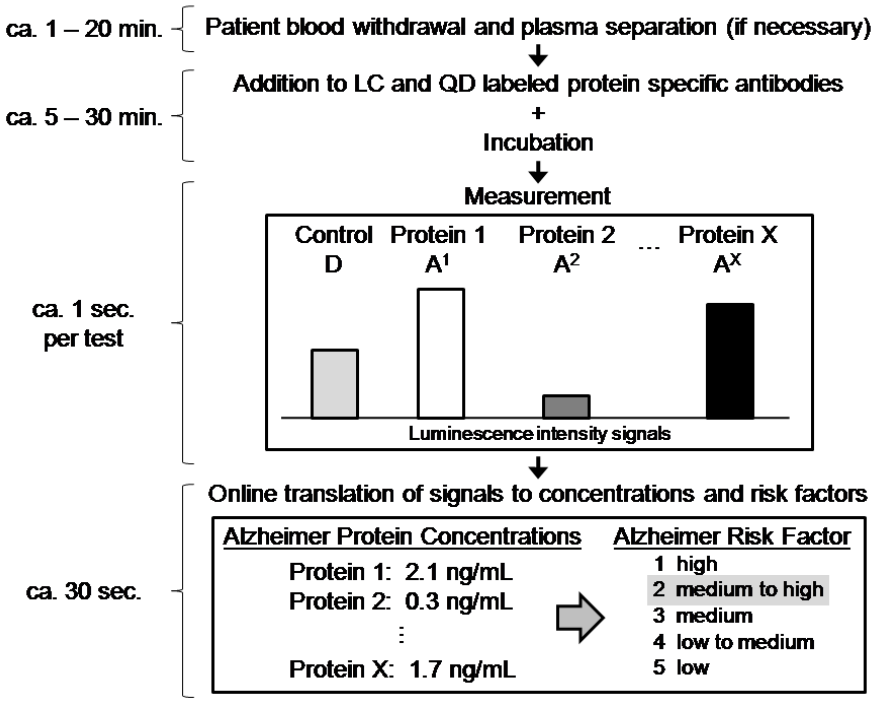

Figure 2: *Different diagnostic steps (+ duration) from blood withdrawal to specific and sensitive diagnosis.*

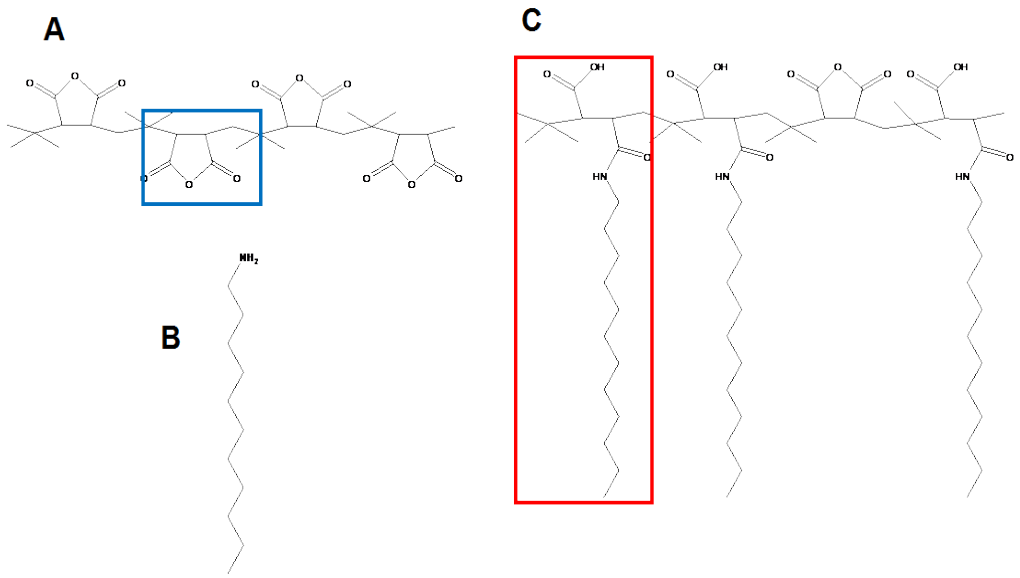

Figure 3: *Molecular structure of the amphiphilic polymer. A) Poly(isobutylene-alt-maleic anhydride). The blue box shows one monomer unit which comprises one anhydride ring. B) Dodecylamine. C) Amphiphilic polymer. 75% of anhydride rings are reacted with a dodecylamine chain. The remaining carboxylic groups stay unreacted and enable both water solubility and the ability of a further functionalization. The red box shows one monomer unit.*

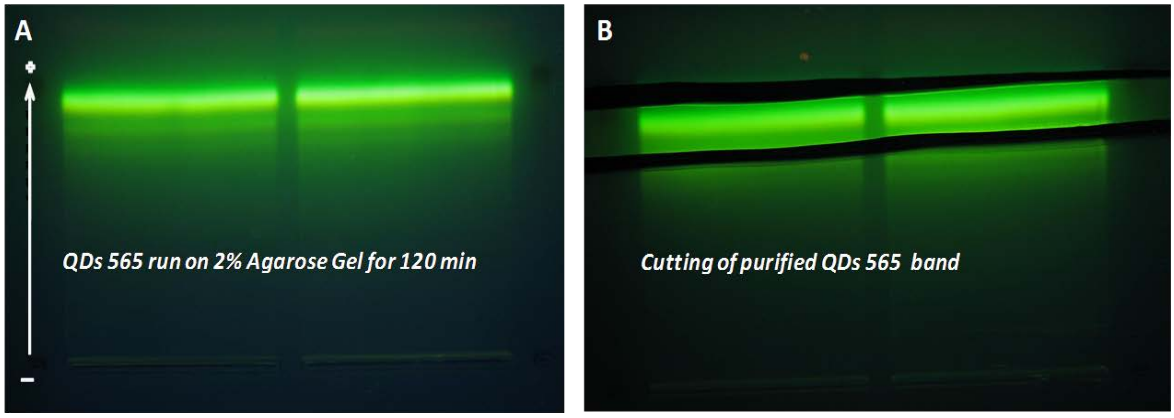

Figure 4: *Gel electrophoresis with QDs emitting at 565 nm. A) QDs were migrating for 120 min in a 2% agarose gel at 10 V/cm. B) After 120 min the required band (free of excess polymer) was extracted.*

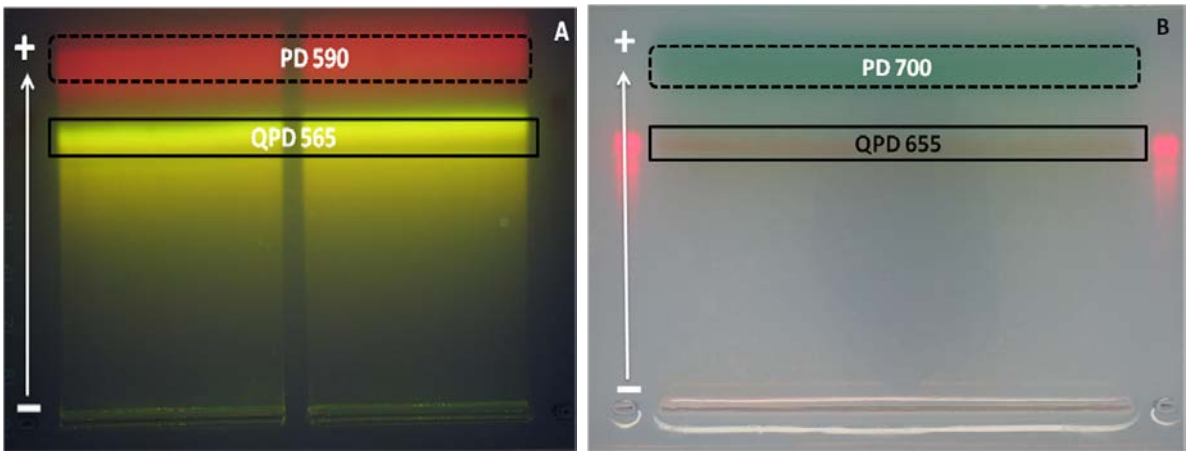

Figure 5: *A) Purification of QDs emitting at 565 nm modified with dye (ATTO-590). The more retarded band QPD (=QDs-polymer-dye) corresponds to purified QDs modified with dye and the faster band PD (=polymer-dye) corresponds to empty polymer micelles. B) Purification of QDs 655 nm modified with dye (DY700).*

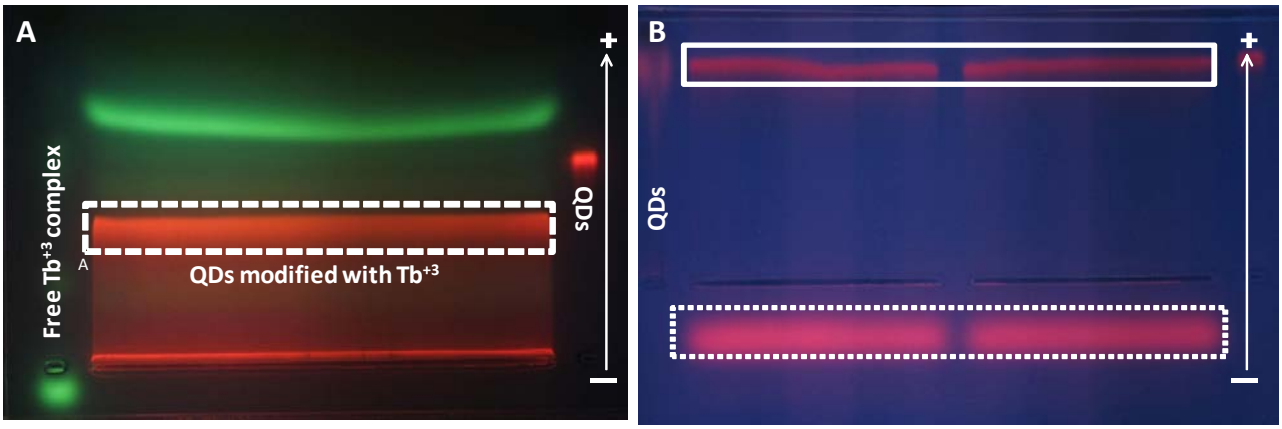

Figure 6: *A) Gel electrophoresis of QDs emitting at 610 nm modified with Tb(III) complex. The dotted band corresponds to QDs modified with Tb(III) complex as compared with controls: QDs and free Tb(III) complex. B) Gel electrophoresis of QDs emitting at 705 nm modified with Eu(III) complex. The slow dotted band corresponds to free Eu(III) complex and the faster band corresponds to Eu(III) modified QDs.*

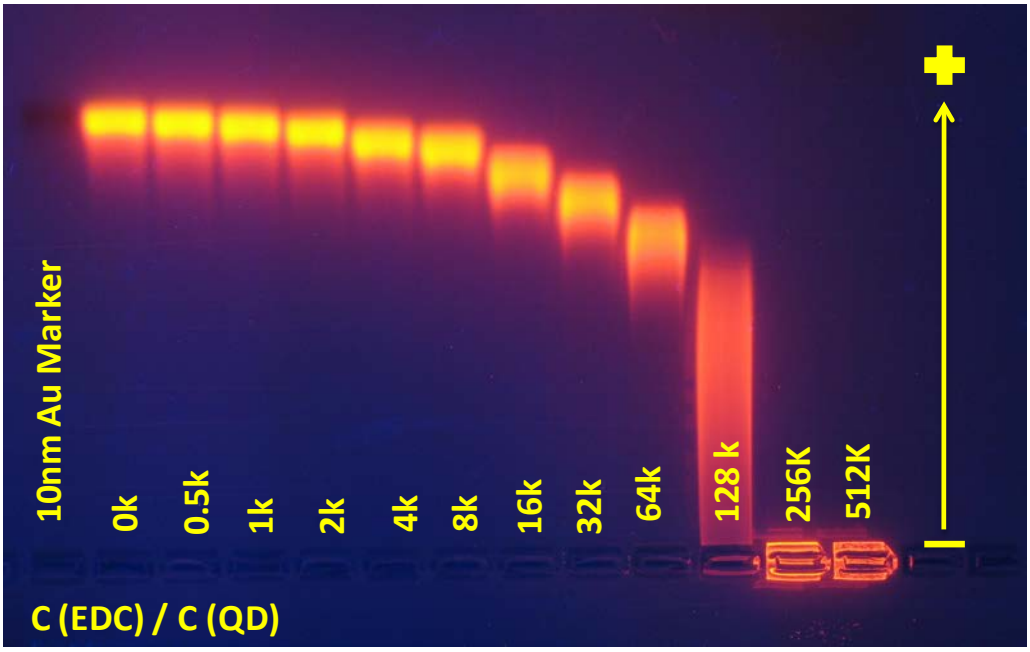

Figure 7: *Test experiment to quantify the amount of EDC per QD required for saturating the QD surface with biotin modified PEG. The columns of the gel correspond to samples with increased EDC concentration from the left to the right. The band with a ratio of 64k PEG molecules per QD looks suitable to saturate the QD surface with PEG under maintained mobility, hence colloidal stability.*

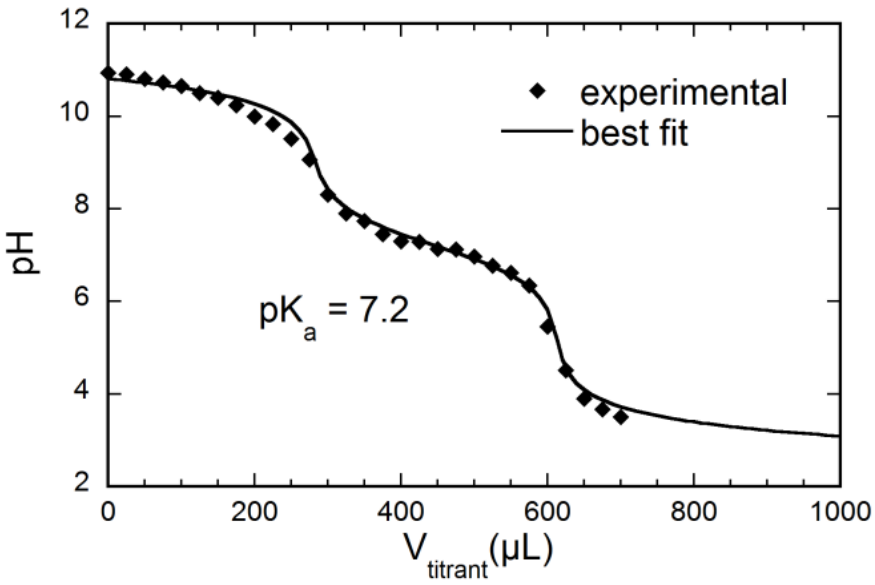

Figure 8: *Experimental titration curve of 7 nm core, polymer coated gold NPs dispersed in 0,7 mM NaOH by HCl and best fit.*

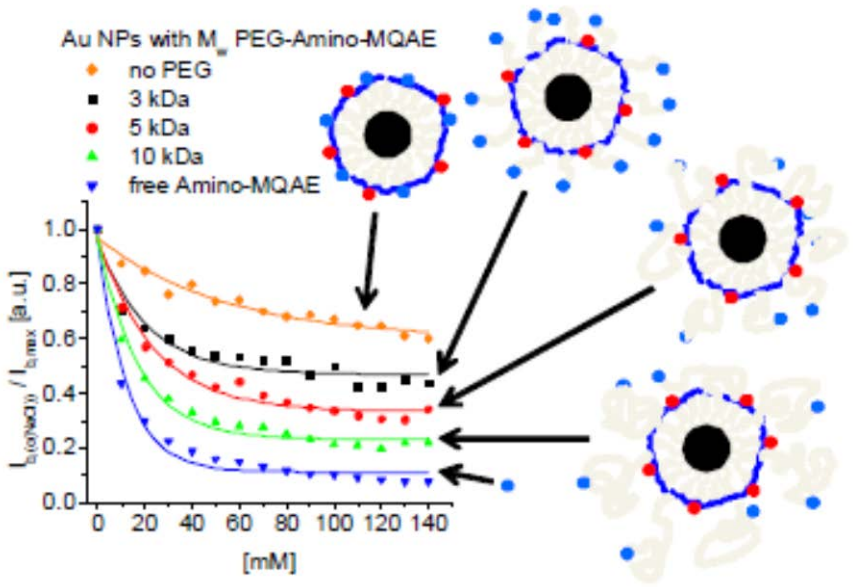

Figure 9: *The maximum emission intensity of Amino-MQAE was plotted against the present NaCl concentration in bulk for various PEG spacers in-between NP surface and fluorophore. In case no PEG is present, thus with the dye directly attached to the polymer shell, the decrease of fluorescence intensity is lower as less chloride ions are present close to the NP surface. In case of PEG spacers with increasing molecular weight (thus length) the fluorescence response is brought closer to the free dye in solution. The spectra were normalized by the cresyl violet (CV, attached to the NP surface) emission maximum and the maximum intensity at 0mM NaCl.*

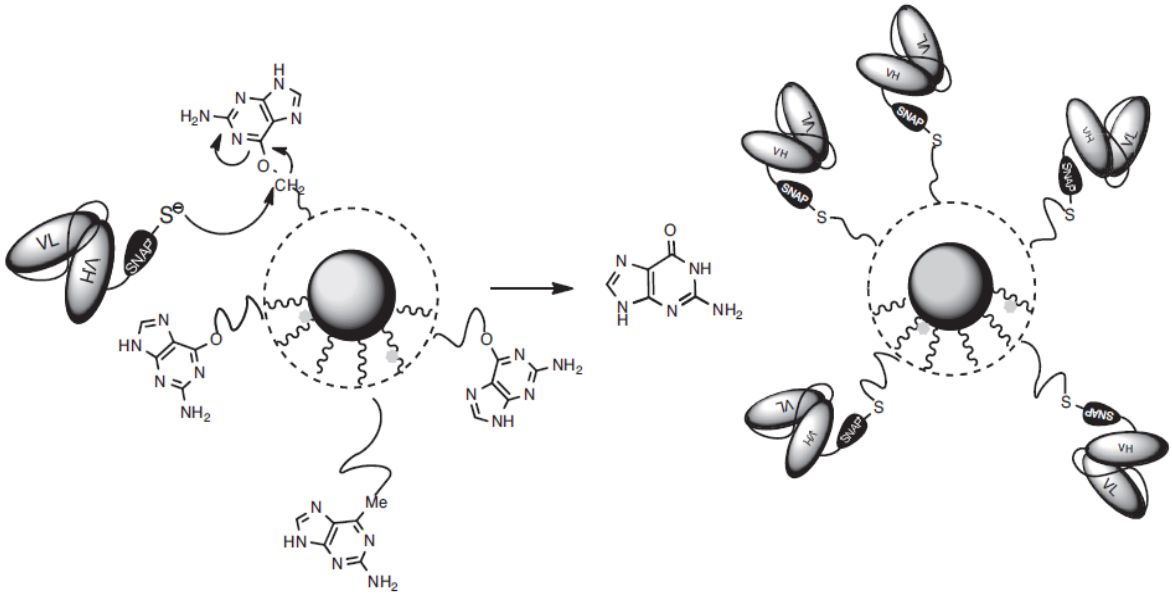

Figure 10: *Conjugation of scFv to the functionalized NPs under release of guanine*

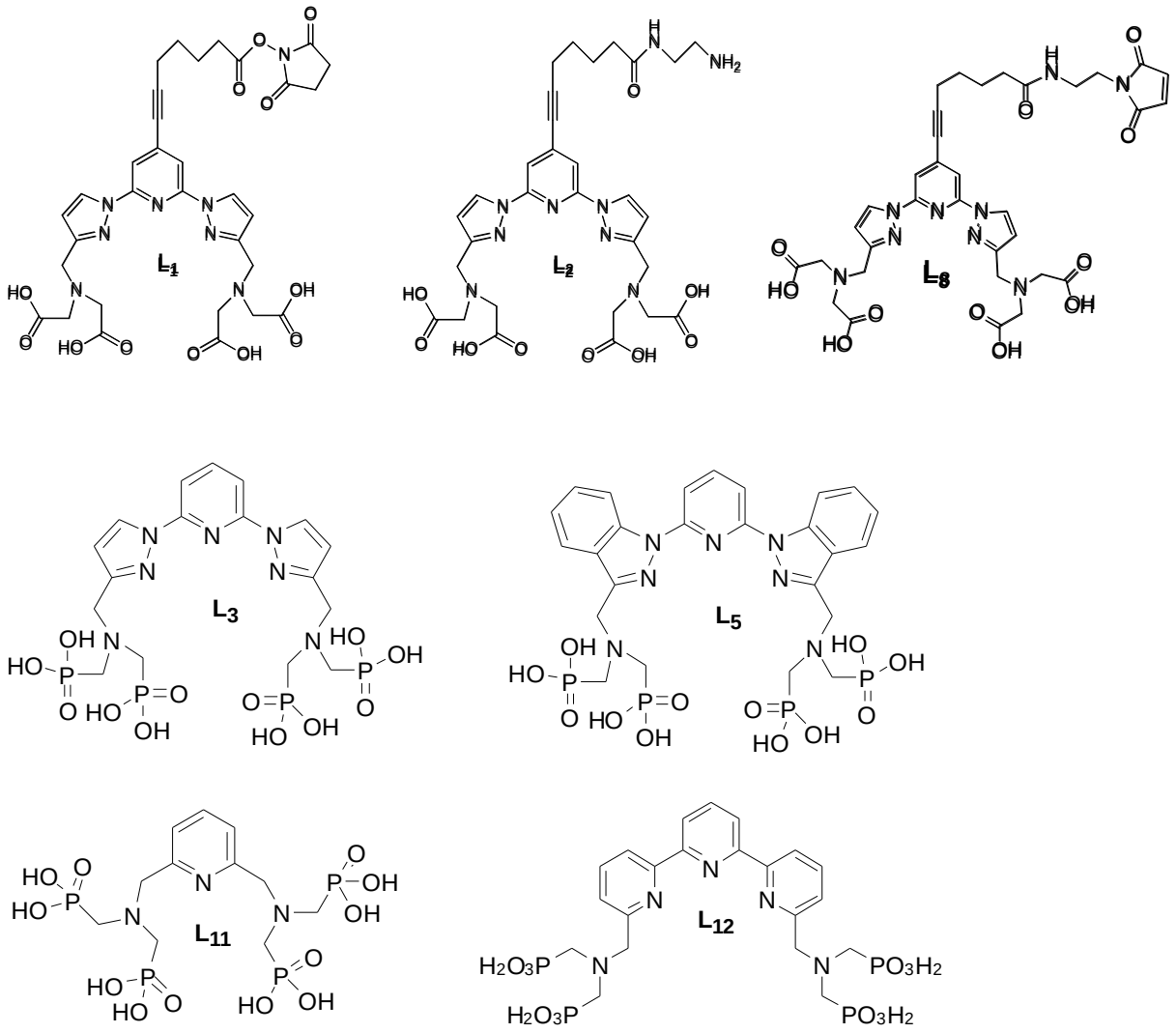

Figure 11: *Synthesized LCs*

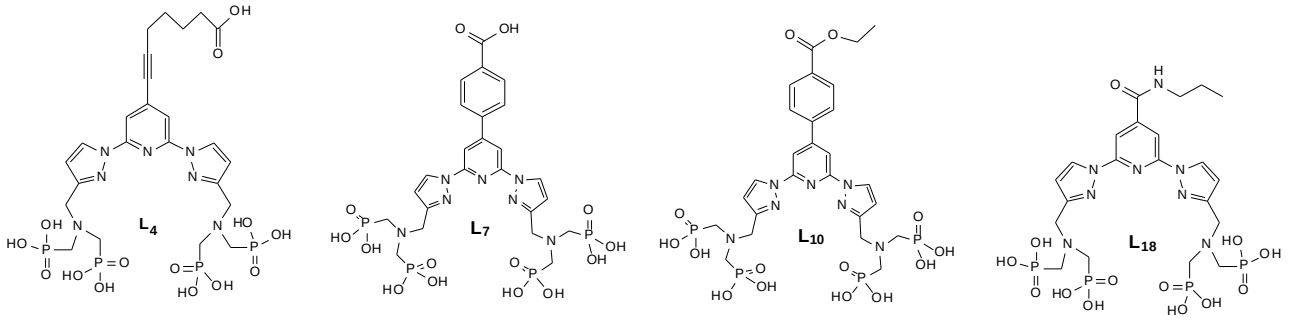

Figure 12: *Modified LCs I*

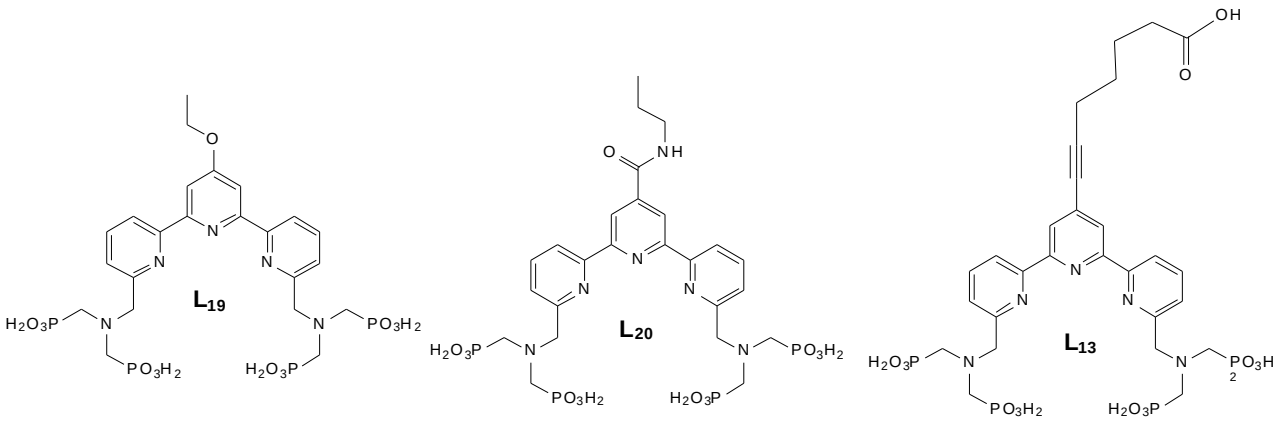

Figure 13a: *Modified LCs II*

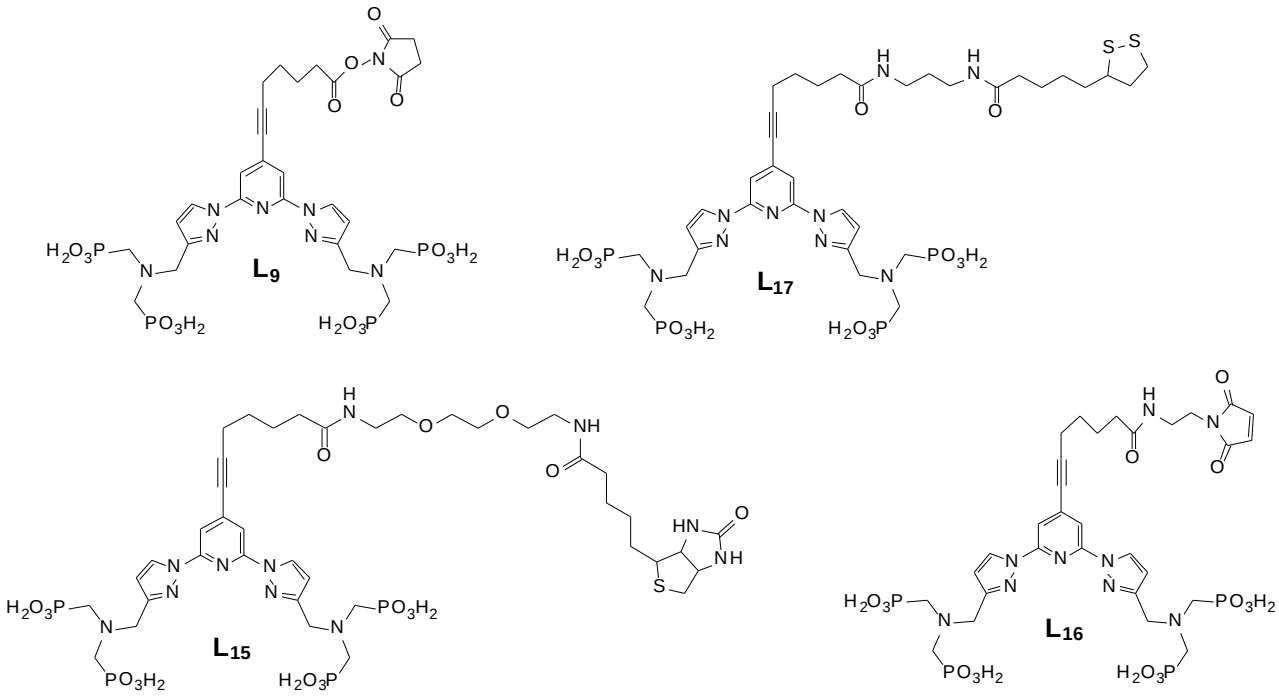

Figure 13b: *LCs with activated function*

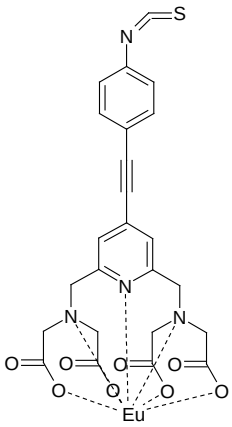

2

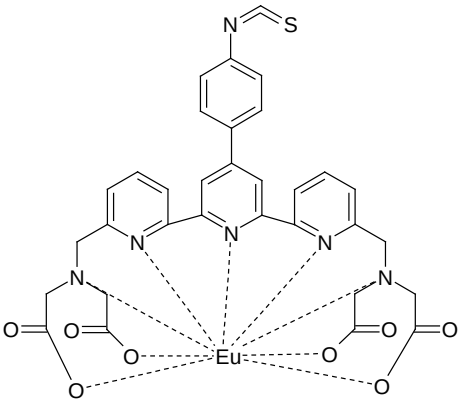

3

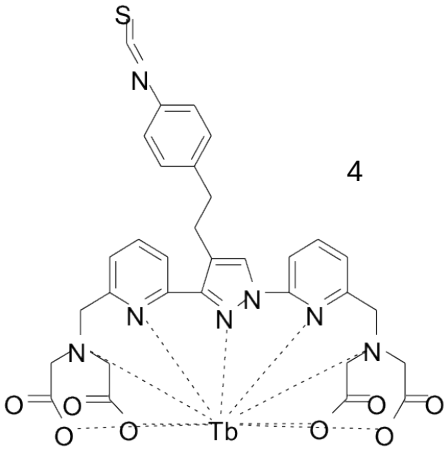

4

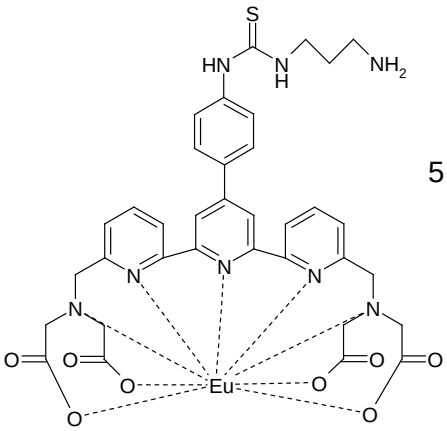

5

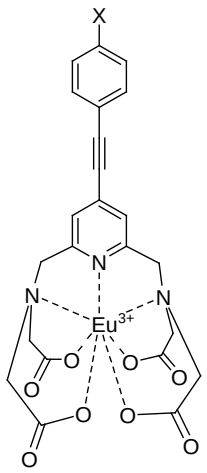

1a,b,c

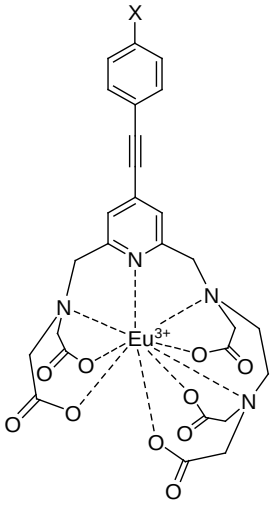

6a,b,c

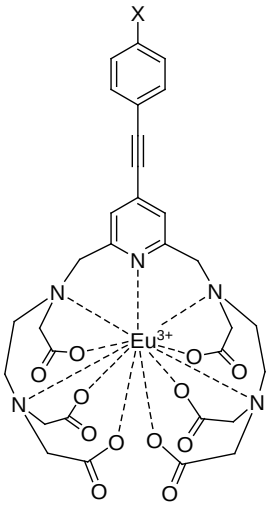

7a,b,c

a: X = NCS
b: X = $NHCSNHCH_2COOH$
c: X = $NHCSNH(CH_2)_3NH$-Biotin

Figure 14: *LCs utilizing novel (1,6,7) and convential (2-5) structures*

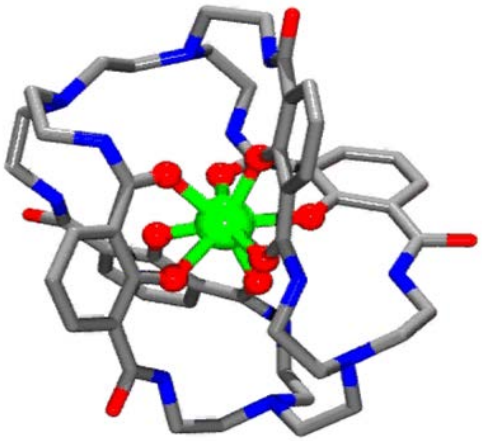

Figure 15: *Lumi4®-Tb complex used for bioconjugation*

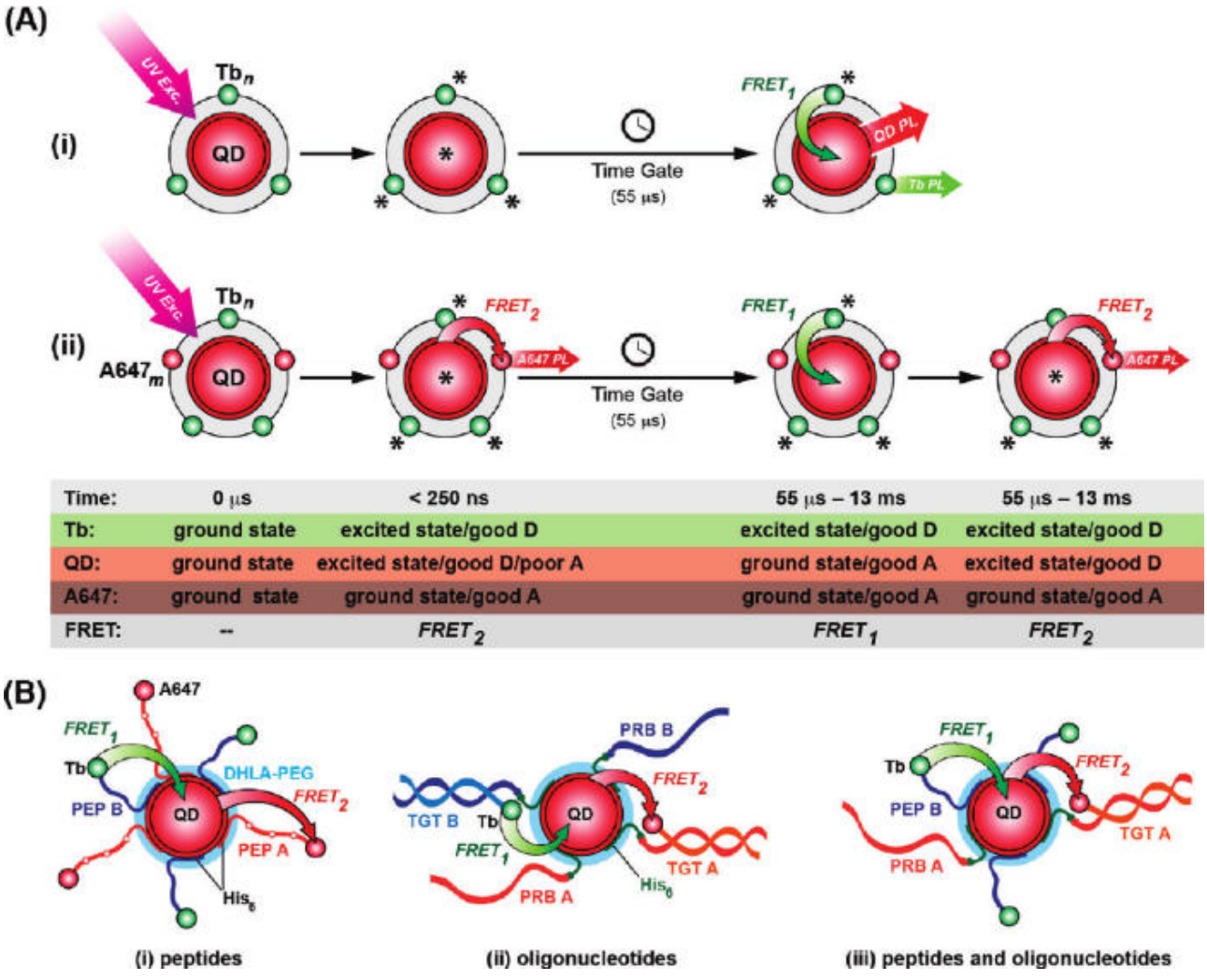

Time:	0 µs	< 250 ns	55 µs – 13 ms	55 µs – 13 ms
Tb:	ground state	excited state/good D	excited state/good D	excited state/good D
QD:	ground state	excited state/good D/poor A	ground state/good A	excited state/good D
A647:	ground state	ground state/good A	ground state/good A	ground state/good A
FRET:	--	FRET$_2$	FRET$_1$	FRET$_2$

Figure 16: *FRET relay system with a QD as simultaneous FRET acceptor and donor*

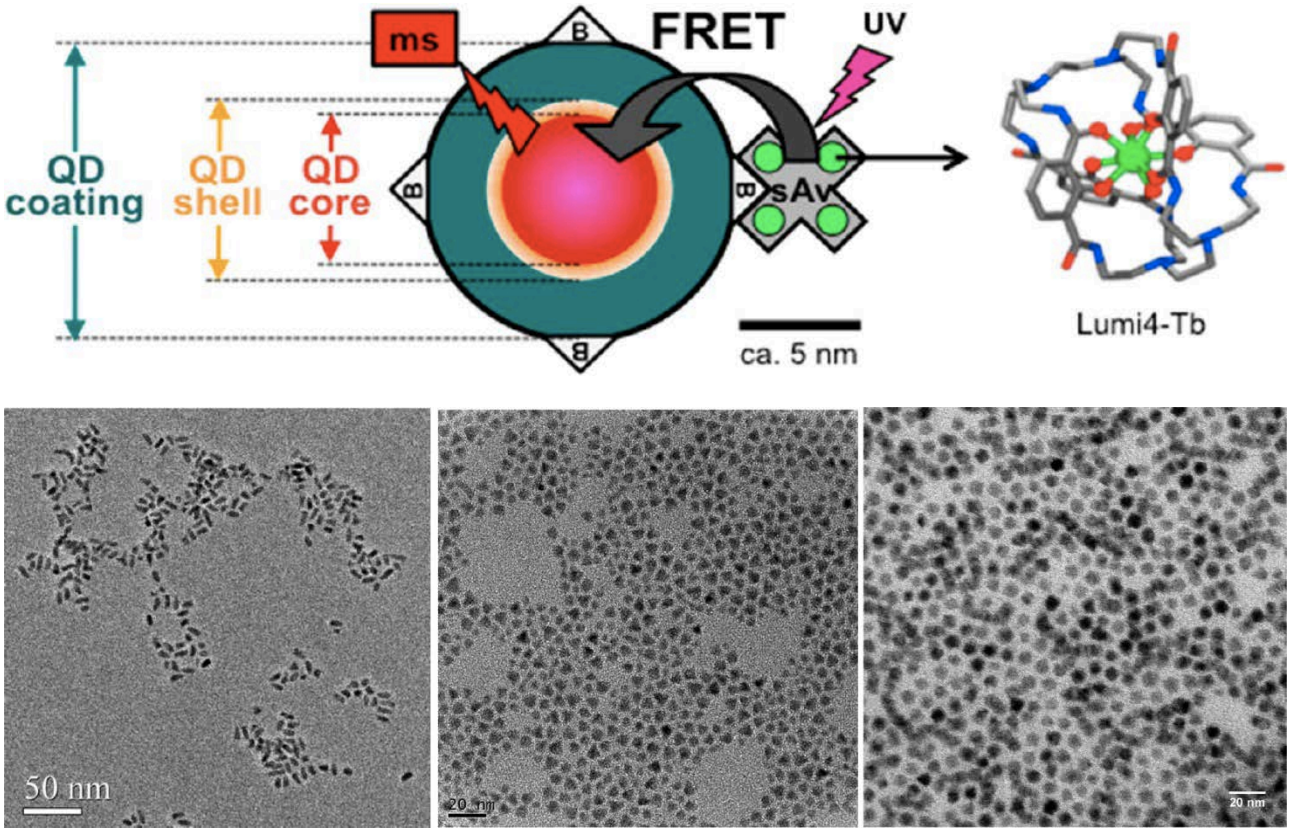

Figure 17: *Time-resolved Tb-to-QD FRET bioassay*

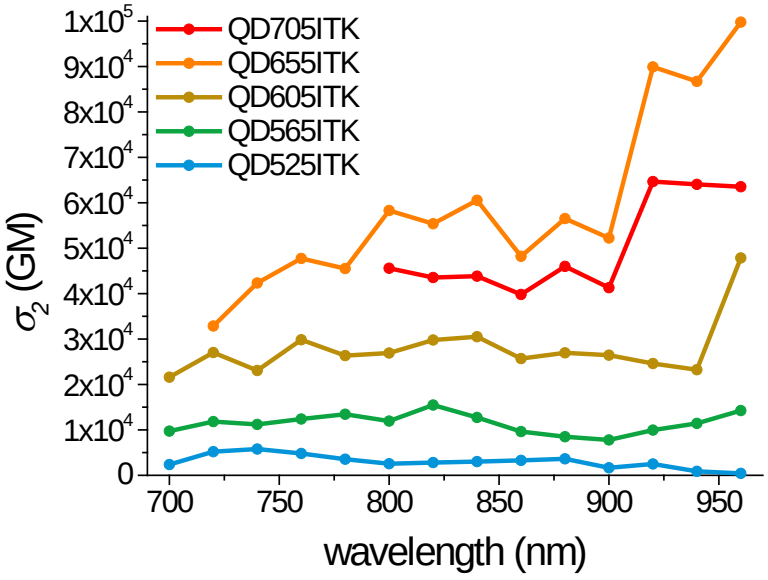

Figure 18: *Plots of the TPE cross-sections (σ_2) for 5 different QDs (525, 565, 605, 655 and 705, Qdot® Nanocrystals – Invitrogen™). ITK (Innovator's Tool Kit) carboxyl quantum dots. The systematic uncertainty in the absolute cross-section values was estimated at ±45%, mostly due to the uncertainty of the fluorescein standard (±30%).*

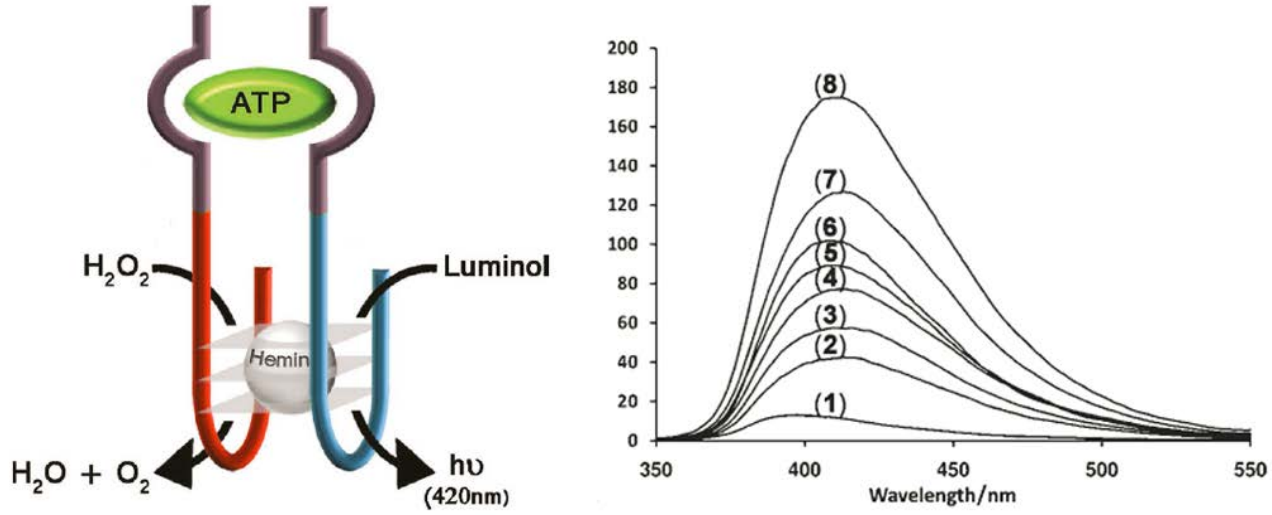

Figure 19: *Analysis of ATP using the CRET-based mechanism resulting upon the formation of a hemin/G-quadruplex CdSe/ZnS functional nanostructure through the self-assembly of an aptamer-ATP complex.*

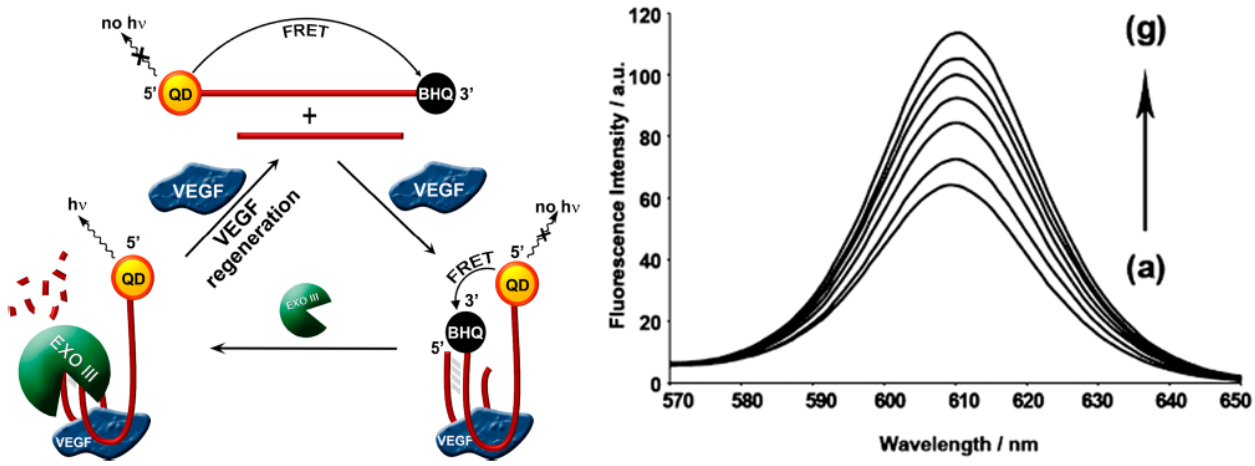

Figure 20: *Amplified FRET-based detection of the VEGF biomarker using Exo III as the VEGF regeneration catalyst.*

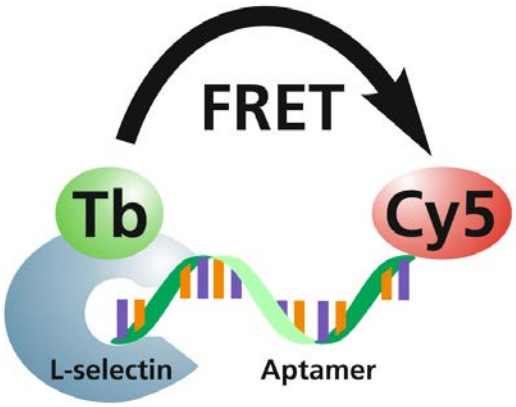

Figure 21: *The architecture of the competitive L-selectin FRET fluoroassay using a Tb-complex-labeled L-selectin and L-selectin-specific aptamer.*

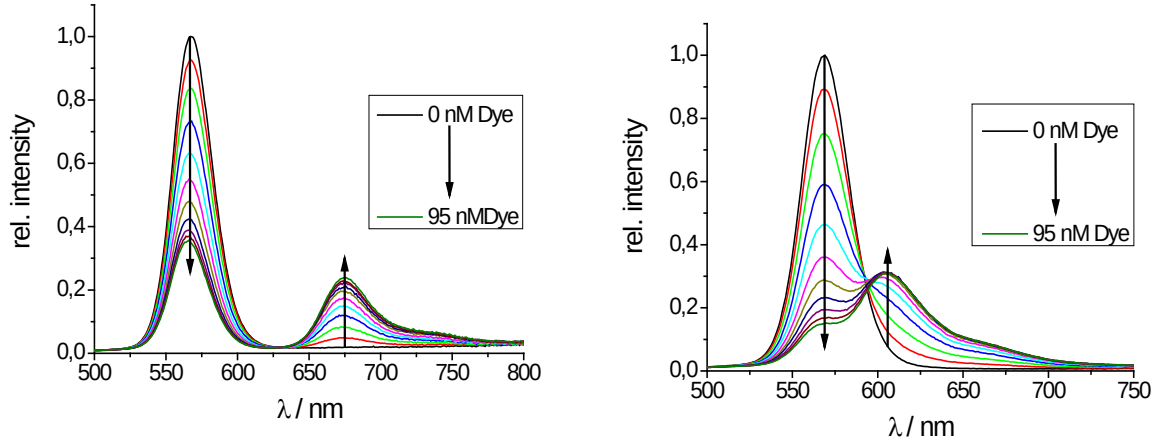

Figure 22: *Steady-state fluorescence spectra of FRET pairs in which to the Biot-QD565 donor AF647 (left) and Strep AF568 (right) was titrated.*

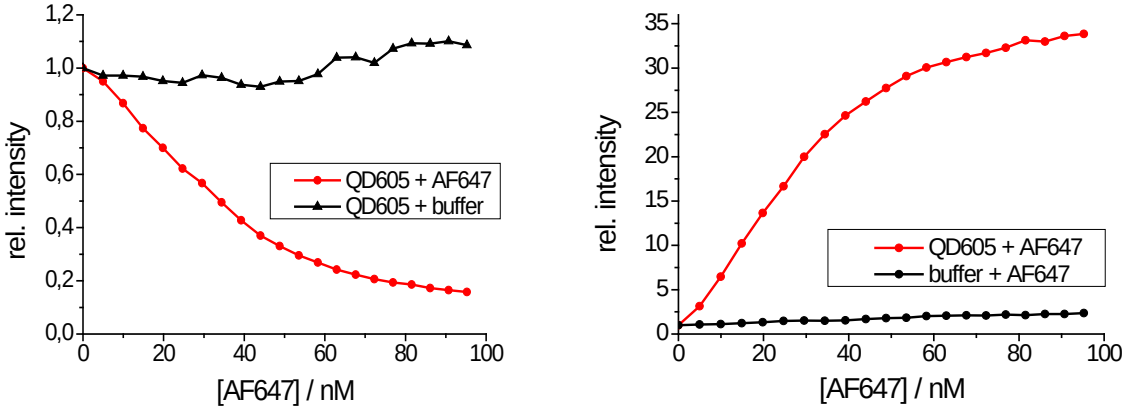

Figure 23: *The relative fluorescence intensity during the titration with acceptor. The signal was collected at donor (left) and acceptor right emission wavelength for Biot-QD605/AF647-Strep system. A curve depicting a titration with pure buffer is added to support FRET occurrence.*

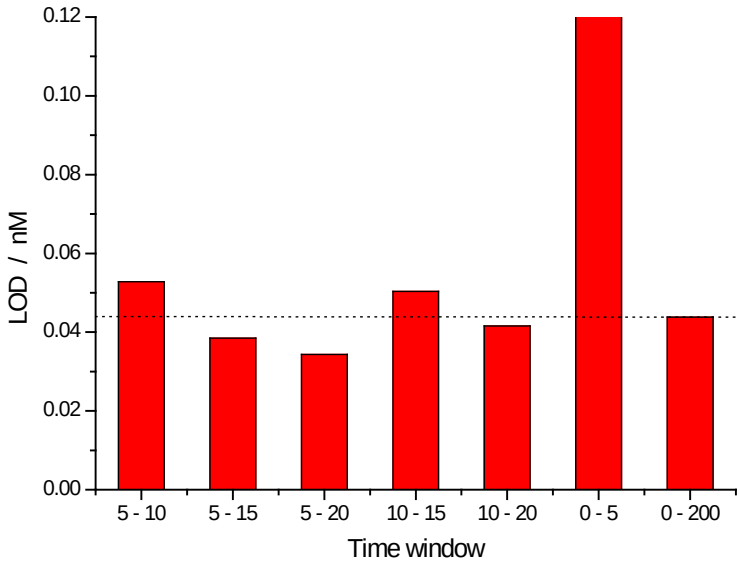

Figure 24: *Limits of detection (LODs) obtained within the different time windows used for the time-gated detection of the Biot-QD605/QF647-Strep FRET assay*

Table 1: *Limits of detection of commercial single assays and crosstalk corrected multiplexed assays, and highest marker concentrations in physiological human serum*

	NSE in pM (ng/ml)	**SCC** in pM (ng/ml)	**CEA** in pM (ng/ml)	**Cyfra21-1** in pM (ng/ml)	**CA15.3** in U/ml[(d)]
LOD commercial single assay[(a)]	10.0 (0.8)	2.1 (0.1)	1.1 (0.2)	5.3 (0.16)	0.3
"common" LOD multiplexing (no other TMs present)	75.0 (6.0)	6.7 (0.32)	0.5 (0.09)	14.3 (0.43)	0.03
"realistic" LOD multiplexing (other TMs present)	150 (12)	18.1 (0.87)	1.1 (0.19)	24.7 (0.74)	0.16
Highest normal concentration[(b)]	156 (12.5)	62.5 (3.0)	27.8 (5.0)	100 (3.0)	30[(c)]

(a) Provided by BRAHMS/Thermo Fisher Scientific for optimized standard clinical KRYPTOR system.
(b) Highest values occurring in healthy persons.
(c) Due to the very high sensitivity of the CA15.3 assay the 1x highest normal concentration in our assays was 30-fold lower (1 U/ml instead of 30 U/ml).
(d) U/ml for CA15.3 cannot be transferred into molar units.

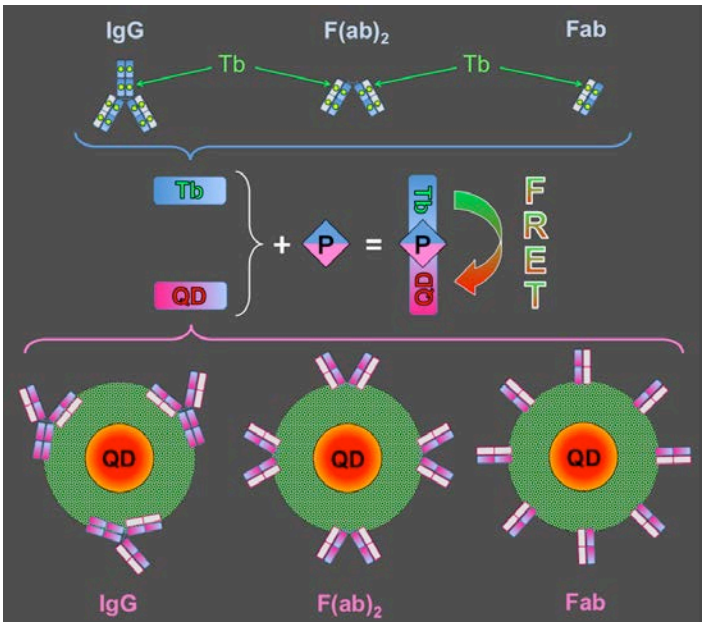

Figure 25: *Principle of the Tb-to-QD FRET-based IgG/F(ab)2/Fab immunoassay*

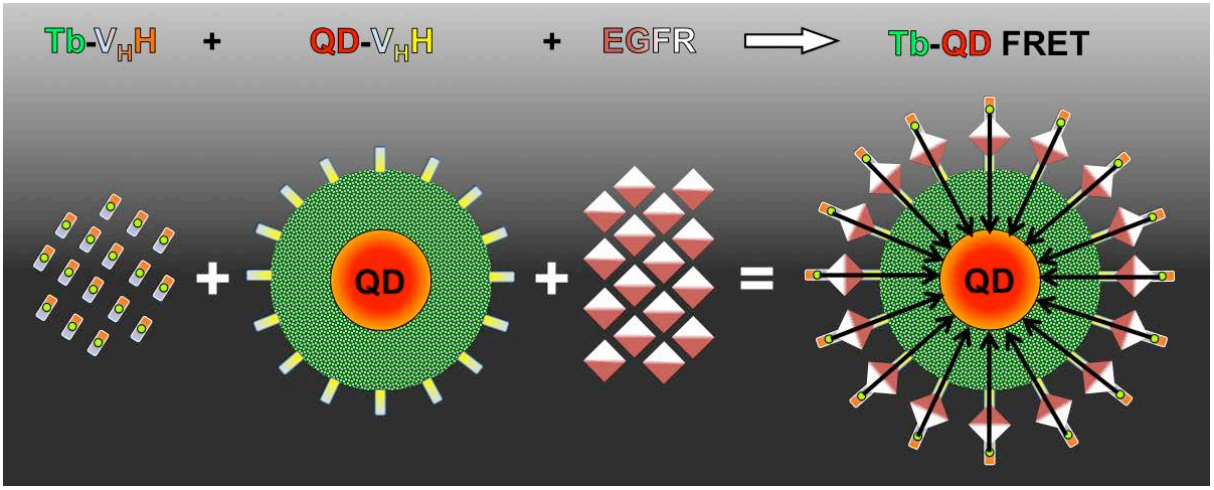

Figure 26: *Principle of the Tb-to-QD FRET-based V_HH immunoassay*

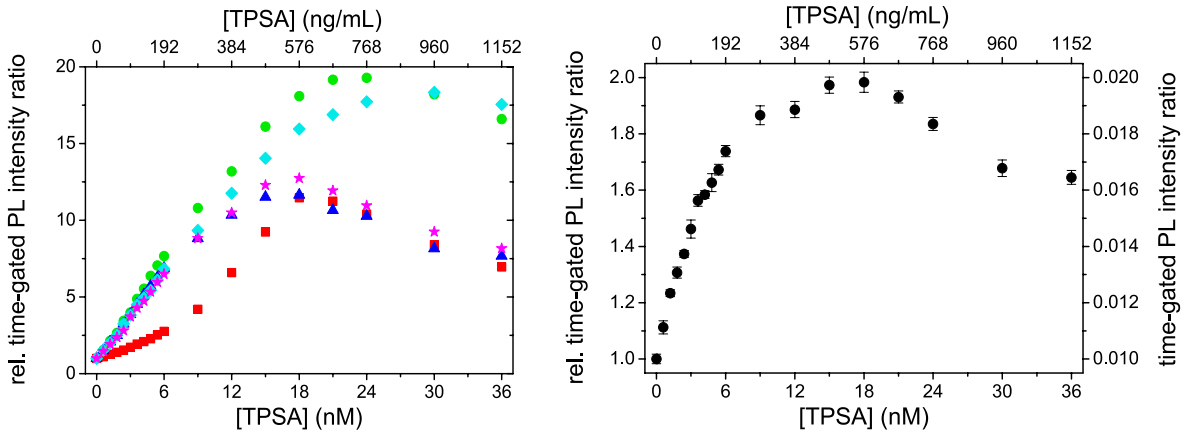

Figure 27: *Tb-to-QD time-gated homogeneous FRET PSA immunoassays using 650nm emitting QDs and 605nm emitting QDs*

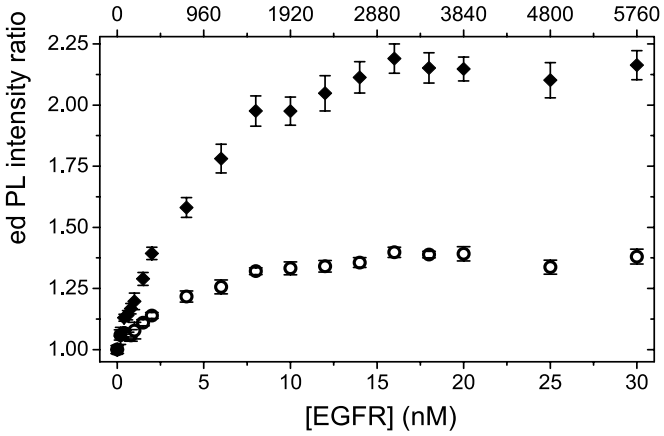

Figure 28: *Tb-to-QD time-gated homogeneous FRET EGFR immunoassays*

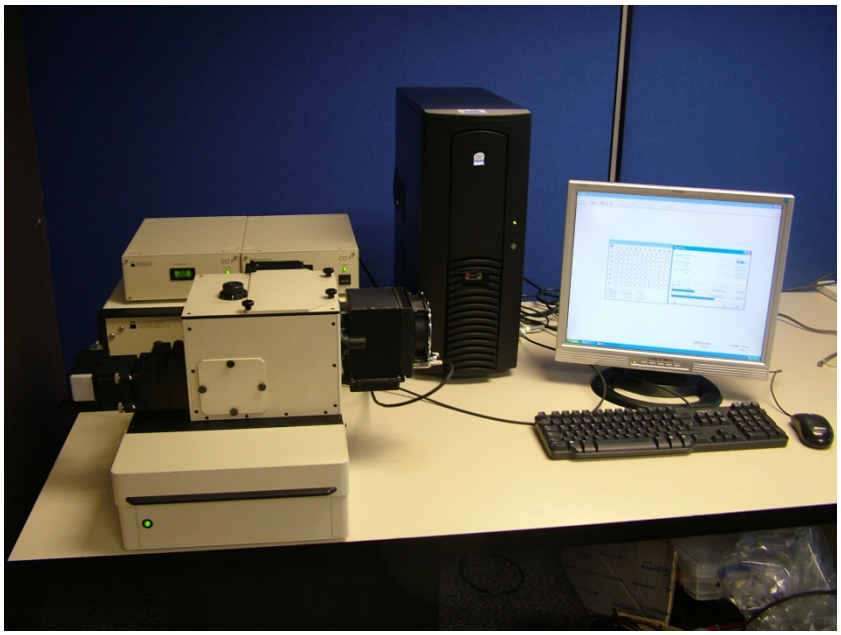

Figure 29: *Multi-modality plate reader*

***Table 2**: Features of the multi-modality plate reader*

Plate Reader	- 96 / 384 well plate - sample volume ca 20-100µl (a relatively low number of patient samples was anticipated with no high throughput screening requirement but sample titrations will be measured)
Excitation Light Source	- interchangeable “plug and play” light sources with variable neutral density filter for power control - microsecond Xenon flashlamp with filter wavelength selection - LED or semiconductor diode laser (c.w. or pulsed) - supercontinuum laser with novel wavelength selector - nitrogen laser or customer supplied light source
Optical Routing Module	- dual channel, confocal design - interchangeable dichroic and wavelength selection filters and polarisers - fibre optic connection to external spectrometer for spectral measurements
Detectors	- dual channel, single photon counting photomultipliers - high gain, red sensitive, Peltier cooled to < - 20^{o}C (<50cps) - electronically gated with selectable gate width
Data Acquisition Electronics	- fast data harvesting acquisition cards for: single photon counting (to 100M cps), multichannel scaling (1µs/channel, optional to 10ns/channel) for microsecond / millisecond range, time correlated single photon counting (TCSPC) for picosecond / nanosecond range
Data Analysis Software	- intuitive, user friendly interface and clear data display - simple colour coded, plate result presentation or sophisticated detailed analysis (including decay analysis up to 4 lifetimes, global analysis, Distribution of Lifetime Analysis, FRET models, anisotropy modules etc.)

Table 3: *Demographic and clinical parameters of health controls, mild cognitive impaired patients, patients with a diagnosis in between MCI and AD and AD patients*

Clinical Diagnosis	**n**	**Age (mean±SD)**	**Sex (%female)**	**MMSE (mean±SD)**
Non-Demented Controls (**NDC**)	21	65 ± 6	61.9	28.9 ± 1.1
Mild Cognitive Impairment (**MCI**)	7	70 ± 8	57.1	28.3 ± 1.3
MCI / AD	3	72 ± 11	33.3	26.3 ± 1.2
Alzheimer Demenz (**AD**)	46	73 ± 9	39.1	21.7 ± 3.1

Table 4: *Number of plasma (EDTA) and CSF samples from healthy controls and patients with MCI, MCI/AD and AD. Normal/pathological of CSF samples according to the results of the Neurochemisches Labor, Universitätsmedizin Göttingen*

Clinical Diagnosis	**n**	**Plasma (EDTA)**	**CSF**	**T-tau, p-tau, Aβ42, Aβ40, Aβ-ratio**
NDC	21	21	17	16 (normal)
MCI	7	7	6	5 (pathological)
MCI / AD	3	3	2	1 (pathological)
AD	46	46	26	24 (pathological)

Reference range*:			
	t-tau	<	450 pg/ml
	p-tau	<	61 pg/ml
	Aβ42	>	450 pg/ml
	Aβ40		no reference range
	Aβ-ratio	>	0.5

*Neurochemisches Labor, Universitätsmedizin Göttingen

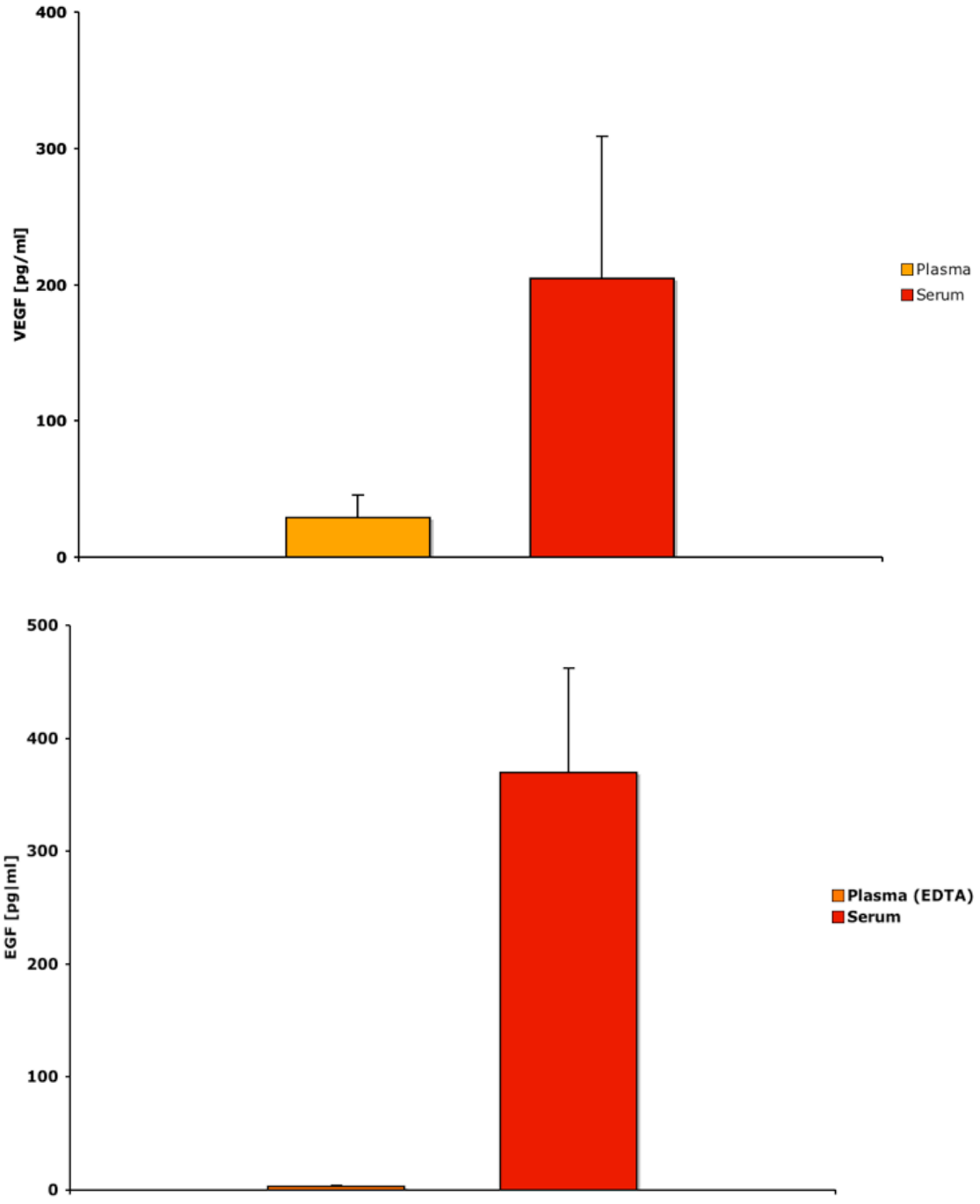

***Figure 30**: VEGF and EGF concentrations in matched pairs of EDTA plasma and serum*

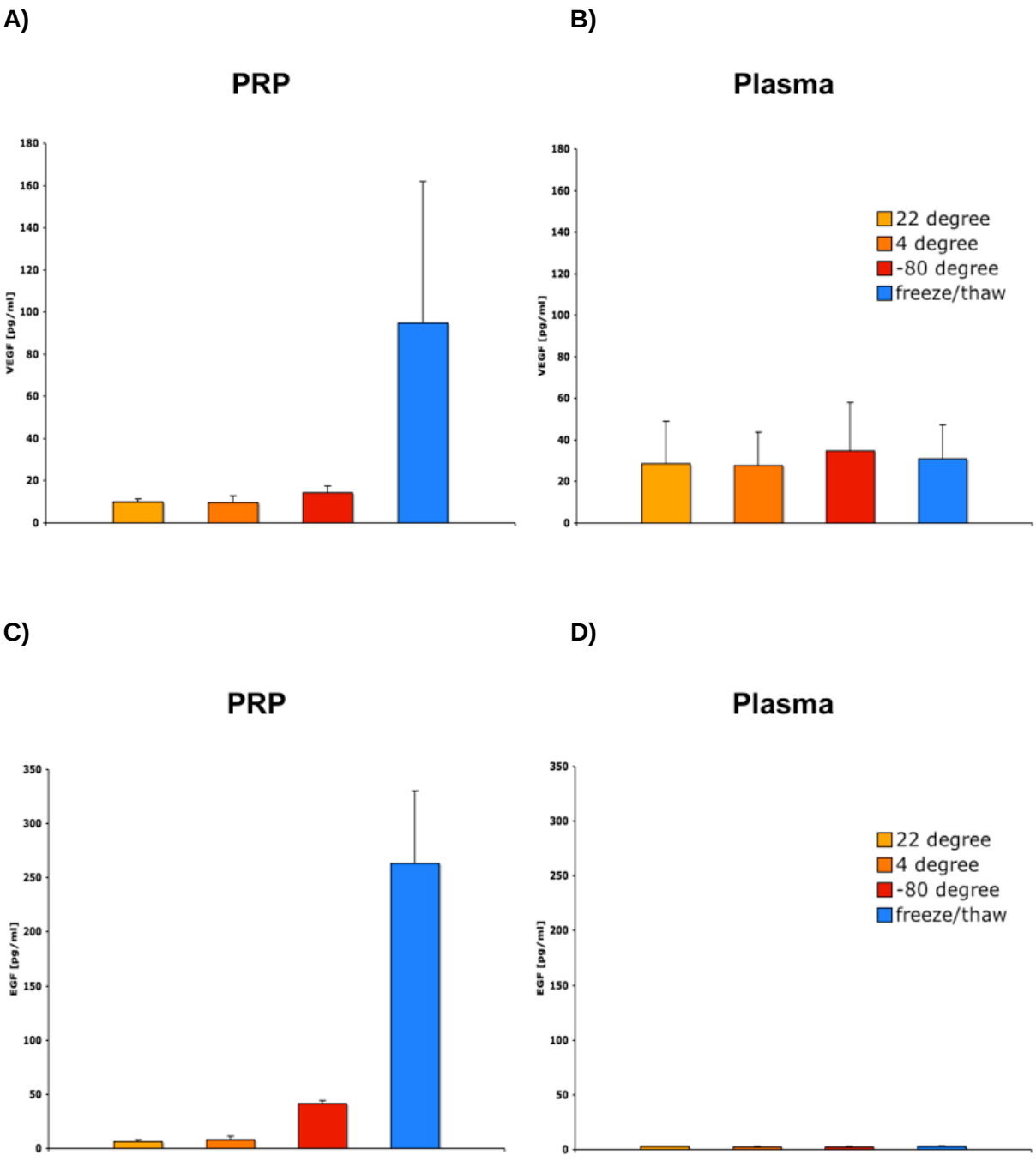

Figure 31: *VEGF and EGF concentrations in relation to storage conditions. Samples stored for 2 hours at 22℃, 4℃ or -80℃. (A) VEGF in platelet rich plasma (PRP). (B) VEGF in plasma. (C) EGF in platelet rich plasma (PRP). (D) EGF in plasma. Positive control: VEGF and EGF concentrations in PRP or plasma after cell rupture by three cycles of freezing and thawing.*

Project logo:

Beneficiaries:

Beneficiary Number *	Beneficiary name	Beneficiary short name	Country	Date enter project	Date exit project
1(coordinator)	Fraunhofer-Gesellschaft zur Förderung der angewandten Forschung e.V.	***Fraunhofer***	Germany	1	42
2	Centre National de la Recherche Scientifique	***CNRS***	France	1	42
3	Universität Potsdam	***UP***	Germany	1	42
4	Philipps Universität Marburg	***PUM***	Germany	1	42
5	The Hebrew University of Jerusalem	***HUJI***	Israel	1	42
6	Charité - Universitätsmedizin Berlin	**Charité**	Germany	1	42
7	Turun Yliopisto	***UTU***	Finland	1	42
8	Edinburgh Instruments Ltd	***EI***	Great Britain	1	42
9	Arctic Photonics Oy	***AP***	Finland	1	20
10	Université Paris-Sud XI	***UPS***	France	13	42